IEEE Access
Multidisciplinary ⋮ Rapid Review ⋮ Open Access Journal

Received 26 March 2023, accepted 14 April 2023, date of publication 19 April 2023, date of current version 27 April 2023.

*Digital Object Identifier 10.1109/ACCESS.2023.3268147*

RESEARCH ARTICLE

# Comparative Design Improvement of the Growing Rod for the Scoliosis Treatment Considering the Mechanical Complications

**UĞUR DEMİR[1], GAZI AKGÜN[1], SITKI KOCAOĞLU[2], MD. ERHAN OKAY[3], AHMED MAJID HEYDAR[4], ERHAN AKDOGAN[5,6], (Member, IEEE), ALPER YILDIRIM[1], SEVDENUR YAZI[7], BORA DEMİRCİ[1], AND ERKAN KAPLANOGLU[8], (Senior Member, IEEE)**

[1]Department of Mechatronics Engineering, Faculty of Technology, Marmara University, 34662 Istanbul, Turkey
[2]Department of Biomedical Engineering, Ankara Yıldırım Beyaz University, 06010 Ankara, Turkey
[3]Department of Orthopaedics and Traumatology, Istanbul Medeniyet University Goztepe Training and Research Hospital, 34722 Istanbul, Turkey
[4]Orthopedic and Traumatology Clinic, Esenyurt Necmi Kadioglu State Hospital, 34517 Istanbul, Turkey
[5]Department of Mechatronics Engineering, Yıldız Technical University, 34349 Istanbul, Turkey
[6]Health Institutes of Türkiye, Istanbul, Turkey
[7]Department of Anatomy, School of Medicine, Marmara University, 34662 Istanbul, Turkey
[8]Department of Engineering Management and Technology, Mechatronics, College of Engineering and Computer Science, The University of Tennessee at Chattanooga, Chattanooga, TN 37403, USA

Corresponding author: Erkan Kaplanoglu (erkan-kaplanoglu@utc.edu)

This work was supported by the Scientific and Technological Research Council of Turkey (TUBITAK) under Project 121E492.

**ABSTRACT** In this study, the focus is on an implant used in the treatment of early-onset scoliosis called magnetically controlled growing rods (MCGR). The primary goal of the study is to address and propose solutions for the mechanical problems reported in the literature concerning MCGR. The problems of the MCGR are mainly due to excessive stress and mechanical bearing problems. Therefore, an MCGR removed from a patient is teardown and geometrically modeled. Then, eleven design parameters are determined on the MCGR for the mechanical problems experienced and these are evaluated by mechanical analysis over 14 control points. In this study, analysis processes are carried out with L12 orthogonal array for eleven design parameters and 2 levels using Taguchi's experimental design method (DoE). With the obtained data by analyzing the experiments in L12, the fitness functions depending on the design parameters are created for 14 control points. Since the problem is multi-objective, a non-dominated sorting genetic algorithm (NSGA II) and multi-objective particle swarm optimization (MOPSO) are used to minimize stress and displacement in existing mechanical problems using fitness functions. The obtained design models from NSGA II and MOPSO are analyzed and evaluated in comparison with the existing mechanical model obtained through pre-optimization teardown study of MCGR.

**INDEX TERMS** Growing rod, mechanical complications, MOPSO, NSGA II, multi-objective optimization.

## I. INTRODUCTION

Scoliosis is a lateral deviation of the spine of more than 10° in the coronal plane. This condition is frequently accompanied by vertebral rotation in the transverse plane and hypokyphosis or lordosis in the sagittal plane [1]. There are four common types of curve patterns, which are thoracic, lumbar, thoracolumbar, and double major. Anteroposterior and lateral X-ray images are taken as a reference for diagnosis. Specific intervention is made based on the Cobb angle measured on the anteroposterior radiograph shown in Figure 1. Treatment modality is determined according to the degree of curvature, skeletal maturity, and risk of progression [2], [3]. In the case of scoliosis with a low Cobb angle, conservative treatment methods such as physical therapy and bracing are used to prevent surgery [1].

The associate editor coordinating the review of this manuscript and approving it for publication was Utku Kose.

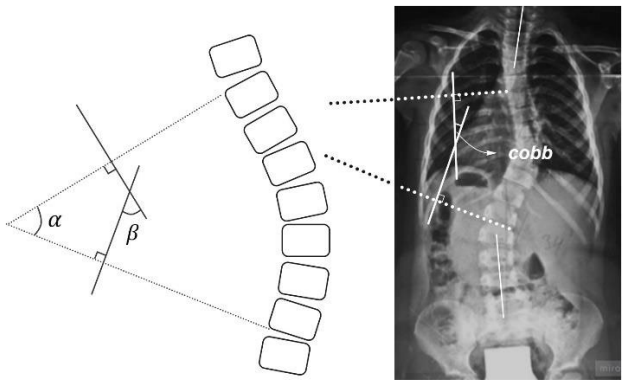


**FIGURE 1.** Cobb angle [19].

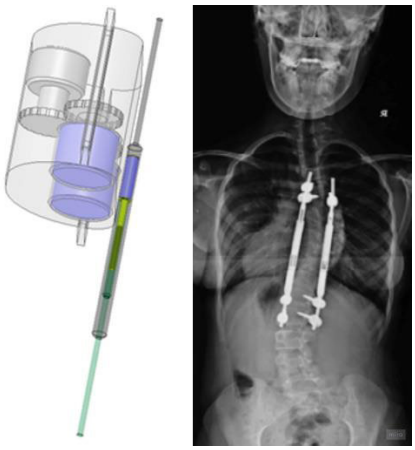

**FIGURE 2.** Double assembly with MAGEC® magnetic rod: external lengthening system, and radiograph of the magnetic rod in the position [19].

Treatment options for scoliosis vary depending on the severity and cause of the condition. Early-onset scoliosis (EOS) presents its own set of challenges, as it begins before the age of 10 years regardless of its [4], [5], [6], [7]. Because of serious problems in lung development, life expectancy significantly reduces in EOS compared to adolescent scoliosis [8]. For this reason, the main goal in the treatment of EOS is to minimize spinal deformity, create a well-developed thoracic cavity, increase lung volume, and maximize pulmonary function [9].

Conventional surgical methods such as spinal fusion, which were preferred for the treatment of EOS in previous periods, give us a great chance to treat spinal deformity but affect pulmonary function and quality of life adversely. Because of the negative effects of conventional surgical methods, new surgical methods such as growing rods have been developed recently [9], [10], [11]. Conventional growing rods and magnetically growing rods are distraction-based and growth-friendly treatment approaches. The main difference between conventional growing rods and magnetically growing rods is repeated anesthesia and open surgical lengthening [9].

Magnetically controlled growing rods (MCGR), the subject of our study, were first reported in the literature as remote-controlled growing spinal instrumentation in 1998 [9], [12]. An initial clinical study of MCGR was performed by [13]. Various structural modifications of the MCGR (insertion of a keeper plate or stainless-steel plate, a smaller-sized actuator for smaller children, reinforcement of the actuator pin, etc.) have occurred since the initial clinical study [14], [15], [16].

MCGR maintains the initial preoperative correction and enhances the spinal growth through outpatient distraction sessions at 2-4 months intervals. Due to non-invasive distraction sessions, MCGR reduces the high complication rate observed in conventional growing rods as much as possible by reducing anesthesia exposure and consequently minimizing surgical scarring, surgical site infection, and psychological distress due to multiple surgeries, improving quality of life, and saving health care costs [9], [17]. Clinical studies evaluating the effectivity of MCGR in patients with EOS have shown that MCGR decreases Cobb angle and increases $T_1$-$T_{12}$ and $T_1$-$S_1$ distances [18], [19]. In addition, it has been reported that the frequent distraction of MCGR stimulates longitudinal vertebral body growth [20], [21].

The MAGEC (MAGnetic Expansion Control) developed by Ellipse company is the only commercialized and clinically available product as shown in Figure 2. Although this system aims to optimize children's scoliosis treatment and additionally increase their quality of life, it has some mechanical and physical complications. One of the serious possible complications of MAGEC is the radiation-related cancers associated with the increased need for radiological imaging during patient follow-up [8], [9].

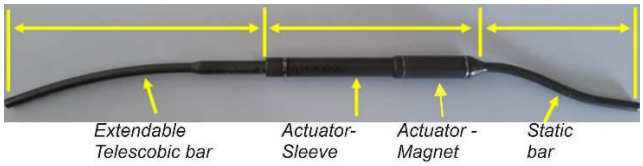


**FIGURE 3.** Teardown Studies and Detailed Component Explanations of MCGR.

A growing rod basically consists of a telescopic (extendable) bar, an actuator, and a static (reference) bar as shown in Figure 3. In this system, the actuator starts rotating as the electromagnetic field is generated with the effect of a permanent magnet (PM) located in the actuator. A screw shaft concentric with the PM, on the other hand, converts the rotational motion into linear motion, allowing the telescopic bar to be elongated [22], [23].

This study aims to find solutions for the mechanical issues reported in the literature by optimizing the mechanical parameters on designated reference planes. The approach taken in this study is to optimize the design parameters collectively, rather than optimizing each parameter individually,

as this could lead to incorrect results. To find the best possible solution, multi-objective optimization is used to optimize all parameters at the same time. The results of this optimization process are represented by a set of non-dominated solutions, also known as the Pareto front. These solutions represent a balance between multiple objectives and are considered to be the Pareto optimal solution in cases where multiple objectives must be considered simultaneously.

In this research, the current mechanical problems of MCGR are tried to improve by the mechanical analysis with intelligent optimization based on multi-objective particle swarm optimization (MOPSO) and non-dominated sorting genetic algorithm II (NSGA II) with Taguchi's design of experiment (DoE).

DoE is a method that is used to determine the relationship between control factors and design parameters. This method determines how much the design parameters change the relevant control factors. It is widely used in the literature to reduce simulation times and costs in optimization processes. In addition, it is seen that it is used to create valuable data sets for data-based optimization and to increase efficiency [24], [25], [26], [27], [28], [29], [30]. In this study, DoE is used to generate datasets and calculate objective functions.

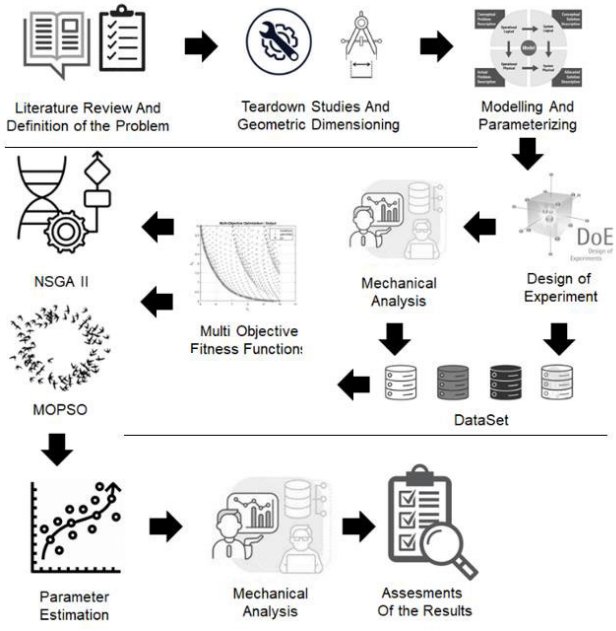


**FIGURE 4.** Process Step of the Methodology.

Particle swarm optimization ensures that randomly generated position and velocity vectors converge to the objective function. The process here is to improve the position of the particles in the solution space, which changes in each iteration. Therefore, it is aimed to determine the optimal position. Similarly, MOPSO tries to provide a non-dominating solution by running the particle swarm optimization algorithm to meet all objective functions and constraints. The algorithm can find a diverse set of solutions by using a concept called "crowding distance" to measure the diversity of solutions in the population and ensure that a wide range of solutions is explored. As a result, MOPSO can identify the non-dominated solutions in the set and generate the Pareto front [31], [32], [33].

NSGA II is used to solve non-convex and discrete multi-objective problems. Its main features are increased convergence, guaranteeing diversity, and non-dominated sorting without the need for constraints [34], [35]. In this study, MOPSO and NSGA II are analyzed comparatively to achieve multi-objective optimization.

## II. MATERIALS AND METHODS

The process steps followed in this study are shown in Figure 4. Firstly, the problem that is commonly encountered in the literature is examined for the MCGR. Then, a teardown study is performed for a growing rod removed from a patient, and both the geometric measurement is performed on the product and the current mechanical problems are observed. After the teardown study, the growing rod is modeled and parameterized. Furthermore, the determined experiments from DoE are analyzed considering the mechanical problems. Multi-objective fitness functions are calculated by evaluating the analysis results. Then, optimization processes are carried out with MOPSO and NSGA II, and the optimal design parameters are tried to be estimated. Finally, mechanical analysis is performed for optimal design parameters, then the results are compared.

### A. THE MECHANICAL COMPLICATIONS OF MCGR

The main problems for the growing rods in the literature are summarized in Table 1. Here, it has been observed that mechanical problems such as rod slippage due to bearing, loss of distraction, formation of abrasion-related debris, rod breakage, actuator locking pin breakage, and abrasion of the gear mechanism.


**FIGURE 5.** Teardown Studies of the MCGR.

### B. TEARDOWN STUDIES

The teardown studies for the MCGR removed from the patient's body after the treatment are given in Figure 5. Here, the geometric measurements are performed for MCGR.

In addition, it is tried to be observed in the mechanical problems that are commonly encountered. It has been observed that the surface of the telescopic bar is abraded by the off axis loads and the deterioration of the bearing.

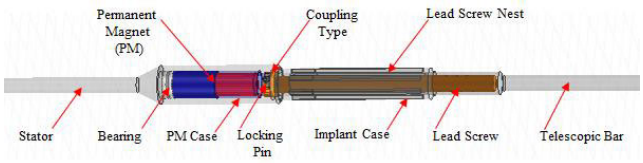


**FIGURE 6.** The CAD model of the MCGR.

### C. MODELLING AND PARAMETERIZING

The obtained geometric dimensions from the teardown study are used to create the CAD model for MCGR as shown in Figure 6. The modeled MCGR consists of sub-components such as stator, telescopic bar, bearing, PM, locking pin, coupling type, leadscrew, and implant case. The MCGR shown in Figure 6 is separated for parametric analysis. Separation into subcomponents is carried out by taking into account the mechanically problematic areas. Thus, the system can be analyzed in eleven parts shown in Figure 7. The abbreviations and explanations of MCGR sub-components are given in Table 2.

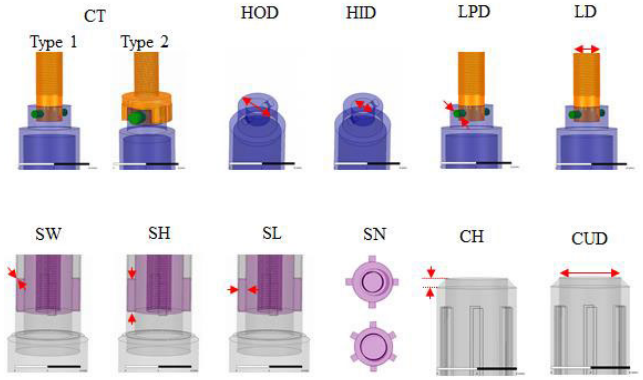


**FIGURE 7.** The Sub-Components of the MCGR.

### D. DESIGN OF EXPERIMENT

In this study, Taguchi's experimental design method is used. So, L12 orthogonal array is chosen for eleven design parameters and two levels referred to as high and low levels. This allows the researcher to test the effect of the factor at two extreme levels. By using only two levels for each factor, the experimental design is simplified and the number of experiments required to identify the optimal combination of input variables is reduced. The experimental design for L12 is formed as given in Table 3.

### E. MECHANICAL ANALYSIS

Basically, seven control points are determined for mechanical analysis. These are locking pin stress (LPS), rod stress (RSS), leadscrew stress (LSS), telescopic bar surface stress (TSS), implant case conical geometry surface stress (ICS), implant case lead nest stress (ILS), x-y axes displacement. (XYD). The control points are shown in Figure 8.

**TABLE 1.** The mechanical complications of MCGR.

| No | Problem | Ref. |
|---|---|---|
| 1 | Rod slippage: As a result of the deformation in the bearing of the telescopic bar with off-axis loads, the torque generated by the actuator is weakened and thus the distraction effect of the rod is lost. | [36,37] |
| 2 | A mismatch between the target and the achieved distraction | [38] |
| 3 | Metaliosis: Metal corrosion resulting in local aseptic fibrosis, local necrosis and loss of implants, and the release of eroding debris products | [39,40] |
| 4 | Breaking rods | [36] |
| 5 | Breaking actuator locking pin | [18,22] |
| 6 | Restriction of the distraction mechanism due to spontaneous bone formation near the actuator unit | [36] |
| 7 | Loss of function of actuator gear mechanism due to deformation | [41] |
| 8 | Proximal anchor loosening | [42] |
| 9 | Due to the thick subcutaneous layer, the distance between the external remote-control device and the internal magnetic increases. This situation decreases the magnetic power that can be transferred to the magnetic rod system. | [37] |
| 10 | Mechanical abrasion: One-sided abrasion is observed on one side of the telescopic bar due to off-axis loading. Consequently, the internal mechanism is weakened. Material loss is observed due to the uncontrolled extension of the telescopic bars in subsequent extension sessions. | [42,43] |

**TABLE 2.** The definition of the sub-components of the MCGR.

| No | Parameters | Abbreviations | Level 1 | Level 2 |
|---|---|---|---|---|
| 1 | Coupling Type (-) | CT | Type 1 | Type 2 |
| 2 | Holder Outer diameter (mm) | HOD | 5 | 6 |
| 3 | Holder Inner Diameter (mm) | HID | 3 | 4 |
| 4 | Locking Pin Diameter (mm) | LPD | 1 | 1.5 |
| 5 | Lead Screw Diameter (mm) | LD | 3 | 4 |
| 6 | Slider Width (mm) | SW | 1 | 1.5 |
| 7 | Slider Height (mm) | SH | 4 | 6 |
| 8 | Slider Depth (mm) | SL | 1 | 0.5 |
| 9 | Slider Number (-) | SN | 4 | 6 |
| 10 | Conical Height (mm) | CH | 0.5 | 1 |
| 11 | Conical Upper Hole Diameter (mm) | CUD | 6 | 6.4 |

**TABLE 3.** L12 Orthogonal array for the MCGR.

| Coded Value According to Levels of the Design Parameters | | | | | | | | | | | |
|---|---|---|---|---|---|---|---|---|---|---|---|
| Exp. No | CT | HOD | HID | LPD | LD | SW | SH | SL | SN | CH | CUD |
| 1 | -1 | -1 | -1 | -1 | -1 | -1 | -1 | -1 | -1 | -1 | -1 |
| 2 | -1 | -1 | -1 | -1 | -1 | 1 | 1 | 1 | 1 | 1 | 1 |
| 3 | -1 | -1 | 1 | 1 | 1 | -1 | -1 | -1 | 1 | 1 | 1 |
| 4 | -1 | 1 | -1 | 1 | 1 | -1 | 1 | 1 | -1 | -1 | 1 |
| 5 | -1 | 1 | 1 | -1 | 1 | 1 | -1 | 1 | -1 | 1 | -1 |
| 6 | -1 | 1 | 1 | 1 | -1 | 1 | 1 | -1 | 1 | -1 | -1 |
| 7 | 1 | -1 | 1 | 1 | -1 | -1 | 1 | 1 | -1 | 1 | -1 |
| 8 | 1 | -1 | 1 | -1 | 1 | 1 | 1 | -1 | -1 | -1 | 1 |
| 9 | 1 | -1 | -1 | 1 | 1 | 1 | -1 | 1 | 1 | -1 | -1 |
| 10 | 1 | 1 | 1 | -1 | -1 | -1 | -1 | 1 | 1 | -1 | 1 |
| 11 | 1 | 1 | -1 | 1 | -1 | 1 | -1 | -1 | -1 | 1 | 1 |
| 12 | 1 | 1 | -1 | -1 | 1 | -1 | 1 | -1 | 1 | 1 | -1 |

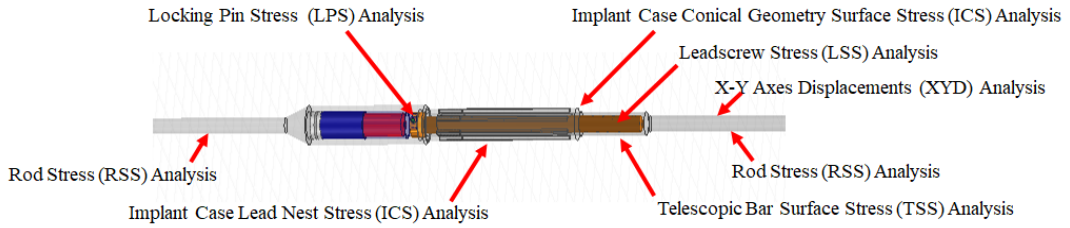


**FIGURE 8.** The Control points for mechanical analysis.

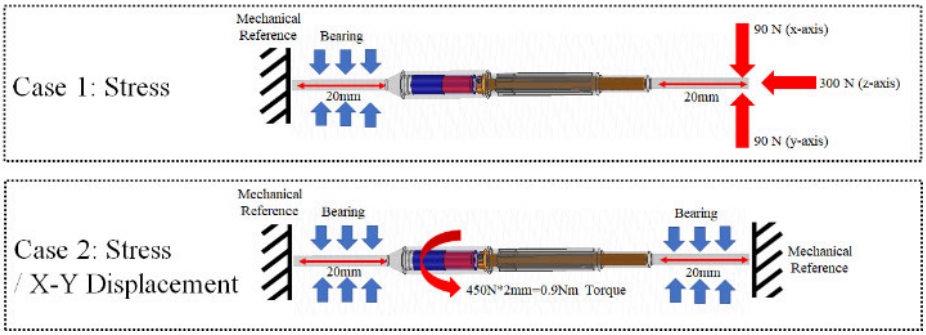


**FIGURE 9.** The analysis case of the mechanical complications.

**TABLE 4.** The optimal design parameters of NSGA II and MOPSO.

| Design Parameters | CT | HOD | HID | LPD | LD | SW | SH | SL | SN | CH | CUD |
|---|---|---|---|---|---|---|---|---|---|---|---|
| NSGA II | 2 | 5.06 | 3.03 | 1.03 | 3.004 | 1.5 | 4.04 | 0.97 | 6 | 1.0 | 6.01 |
| MOPSO | 2 | 5.83 | 3 | 1 | 3 | 1 | 5 | 0.683 | 5 | 0.904 | 6.001 |

The mechanical loads experienced by MCGR were analyzed by conducting static analyses. Static analysis studies were conducted using SOLIDWORKS Simulation Premium. The boundary conditions applied in the static analysis are shown in Figure 9. The Von-Mises stresses and deformation results that occurred in the system were examined as a result of the analysis.

Here, 2 cases can be considered for the control points except for x-y axis displacement. These control points represent axial and off-axis loadings. In addition, it is necessary to analyze the stress that will occur due to torque during the operation of the MCGR. Considering all these, the analyzes given in Figure 9 should be performed.

On the other hand, case 2 given in Figure 9 is performed for x-y axes displacement. Considering all cases and control points, the fourteen control factors should be analyzed for the DoE shown in Table 3.

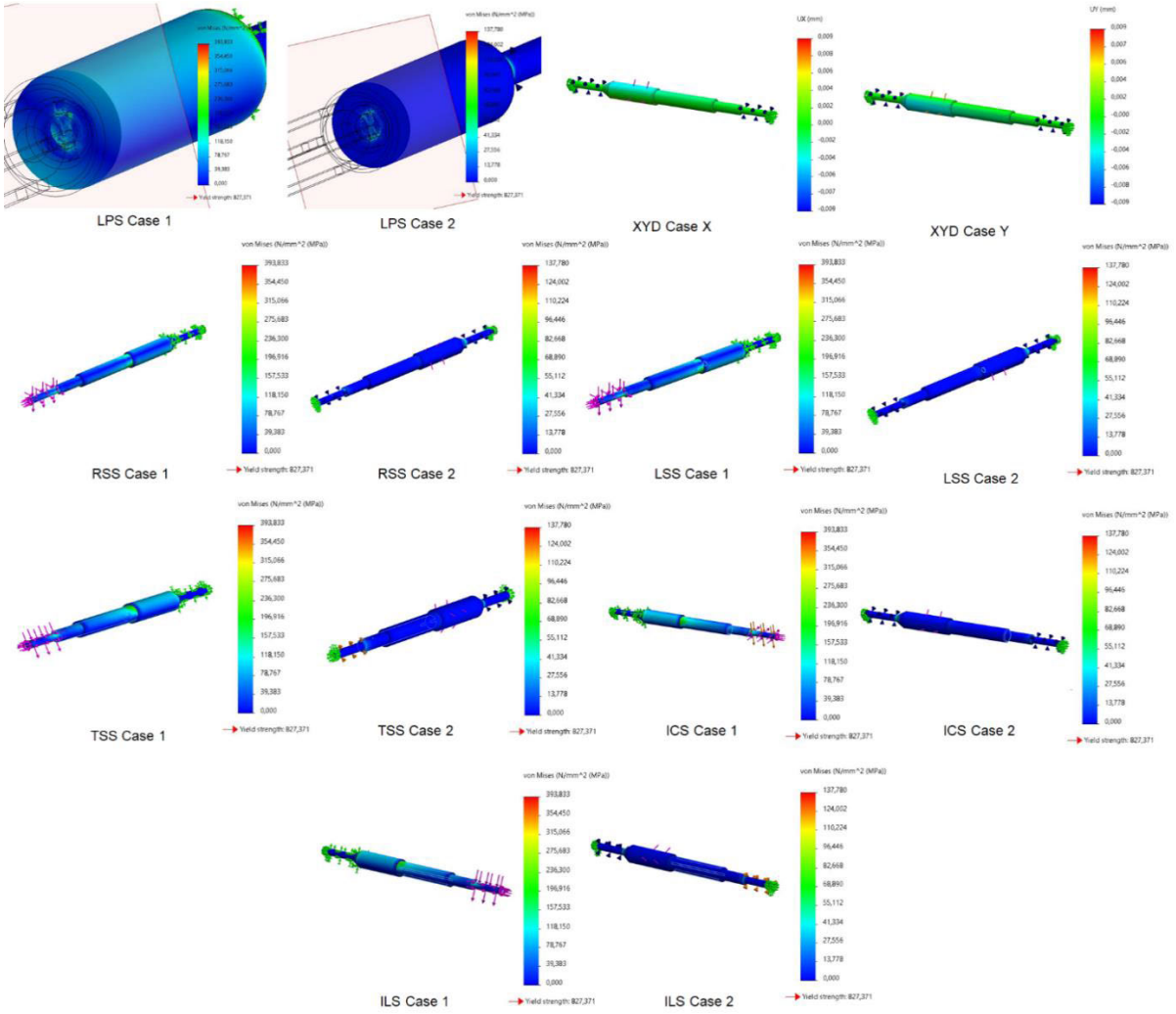


**FIGURE 10.** The analysis results of L12 Exp.1.

**TABLE 5.** The analysis results of NSGA II.

| LPS C.1 | LPS C.2 | ICS C.1 | ICS C.2 | TSS C.1 | TSS C.2 | LSS C.1 | LSS C.2 | ILS C.1 | ILS C.2 | RSS C.1 | RSS C.2 | XYD C.X | XYD C.Y |
|---|---|---|---|---|---|---|---|---|---|---|---|---|---|
| (MPa) | (MPa) | (MPa) | (MPa) | (MPa) | (MPa) | (MPa) | (MPa) | (MPa) | (MPa) | (MPa) | (MPa) | (mm) | (mm) |
| 67.79 | 44.77 | 195.78 | 3.98 | 195.6 | 10.61 | 66.97 | 15.17 | 210.7 | 8.96 | 227.5 | 70.9 | 0.027 | 0.027 |

### F. MULTI-OBJECTIVE FITNESS FUNCTION

In this study, the fitness functions are obtained with linear regression as given in equation (1). The coefficients ($\beta_{i_k}$) given in equation (2) are calculated for 14 control points.

$$F_f = \begin{pmatrix} F_{LPS_{Case_1}}, F_{LPS_{Case_2}}, F_{ICS_{Case_1}}, F_{ICS_{Case_2}}, F_{TSS_{Case_1}}, \\ F_{TSS_{Case_2}}, F_{LSS_{Case_1}}, F_{LSS_{Case_2}}, F_{ILS_{Case_1}}, F_{ILS_{Case_2}} \\ , F_{RSS_{Case_1}}, F_{RSS_{Case_2}}, F_{XYD_x}, F_{XYD_y} \end{pmatrix} \tag{1}$$

Here, $F_f$ is fitness functions vector of all cases as first and second case of LPS, RSS, LSS, TSS, ICS, ILS, and XYD.

$$F(F_f) = \sum_{k=1}^{14} \begin{bmatrix} \beta_{0_k} + \beta_{1_k}.CT + \beta_{2_k}.HOD \\ +\beta_{3_k}.HID + \beta_{4_k}.LPD + \beta_{5_k}.LD \\ +\beta_{6_k}.SW + \beta_{7_k}.SH + \beta_{8_k}.SL \\ +\beta_{9_k}.SN + \beta_{10_k}.CH + \beta_{11_k}.CUD + \varepsilon_{0_k} \end{bmatrix} \tag{2}$$

**TABLE 6.** The analysis results of NSGA II.

| LPS C.1 | LPS C.2 | ICS C.1 | ICS C.2 | TSS C.1 | TSS C.2 | LSS C.1 | LSS C.2 | ILS C.1 | ILS C.2 | RSS C.1 | RSS C.2 | XYD C.X | XYD C.Y |
|---|---|---|---|---|---|---|---|---|---|---|---|---|---|
| (MPa) | (MPa) | (MPa) | (MPa) | (MPa) | (MPa) | (MPa) | (MPa) | (MPa) | (MPa) | (MPa) | (MPa) | (mm) | (mm) |
| 56.05 | 52.68 | 208.94 | 4.27 | 196.1 | 10.68 | 71.82 | 15.58 | 211.1 | 9.08 | 227.5 | 70.7 | 0.027 | 0.027 |

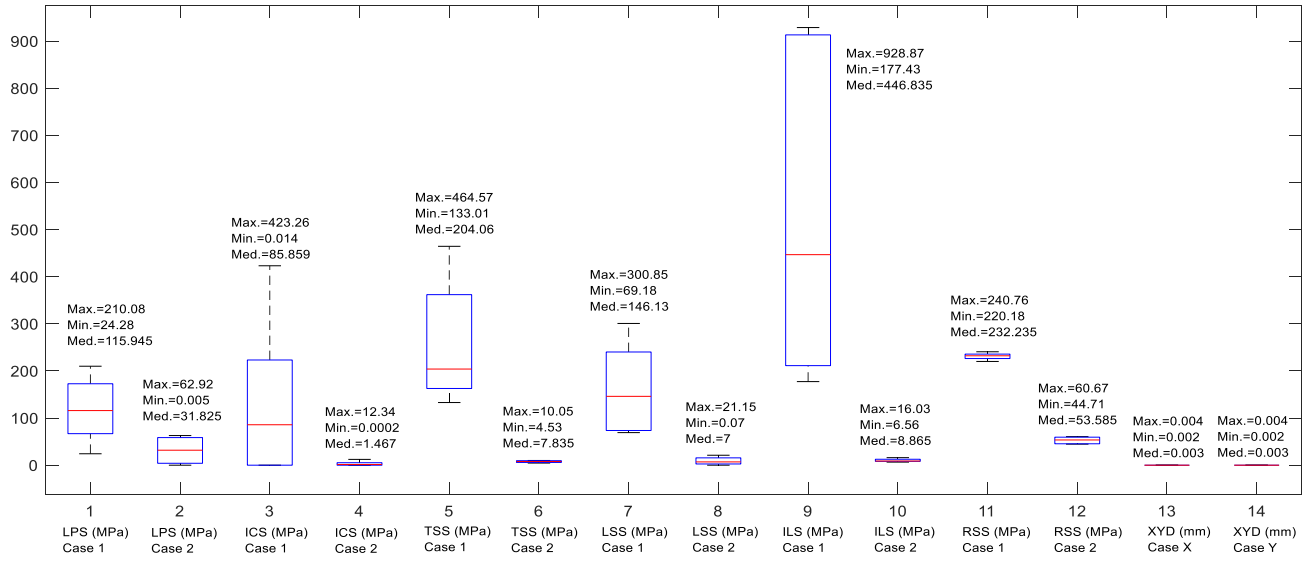


**FIGURE 11.** The analysis results of the mechanical complications.

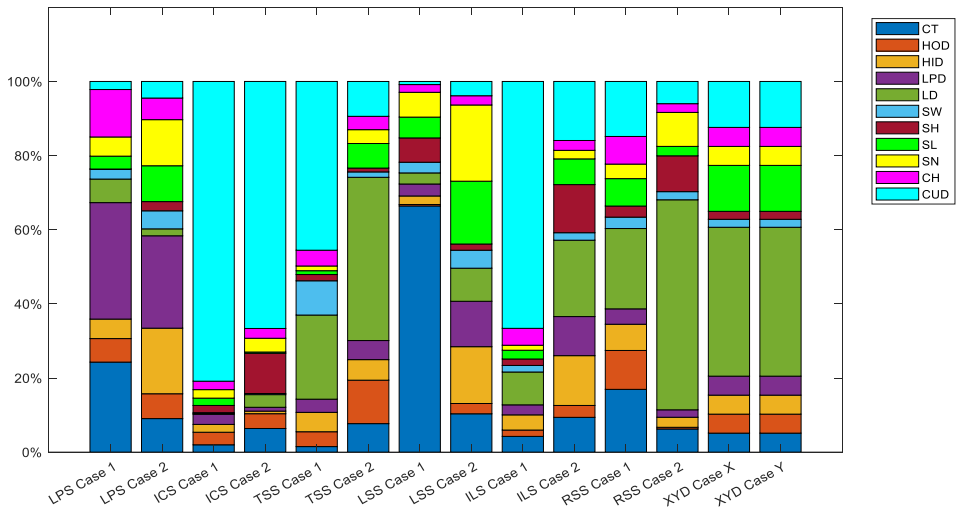


**FIGURE 12.** The ranking of the design parameters according to DoE.

### G. OPTIMIZATION ALGORITHM

This study aims to minimize the stress values and displacement in the x-y axes. Therefore, both NSGA II and MOPSO are run to obtain the optimal design parameters for fourteen control points. The optimization algorithm is defined as follows.

OBJECTIVE

$$Minimize : F\left(F_f\right) \tag{3}$$

SUBJECT TO

$$\left(F_f\right) \leq Median\left(F_f\right) \tag{4}$$

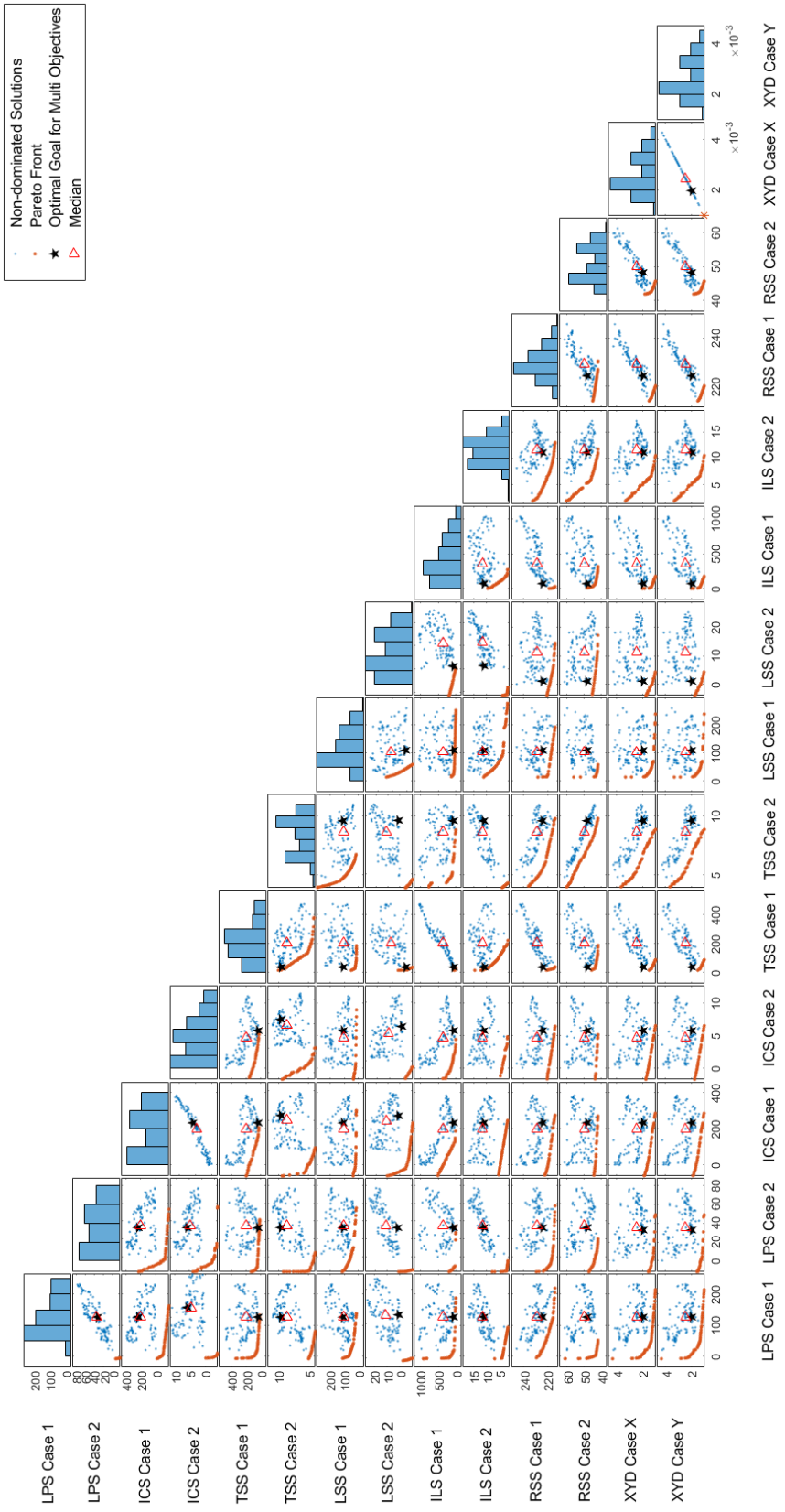


**FIGURE 13.** Plot matrix of NSGA II.

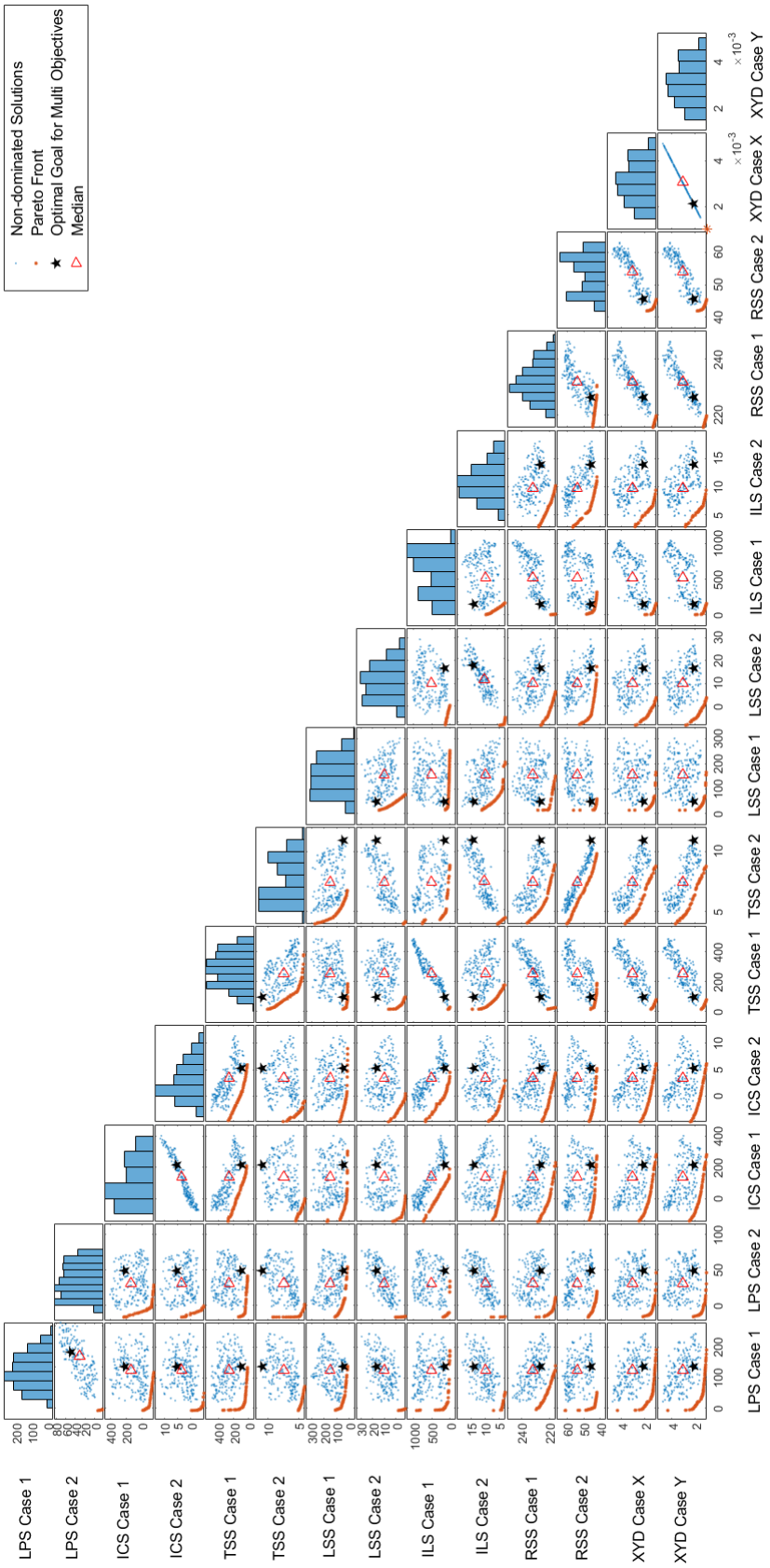


**FIGURE 14.** Plot matrix of MOPSO.

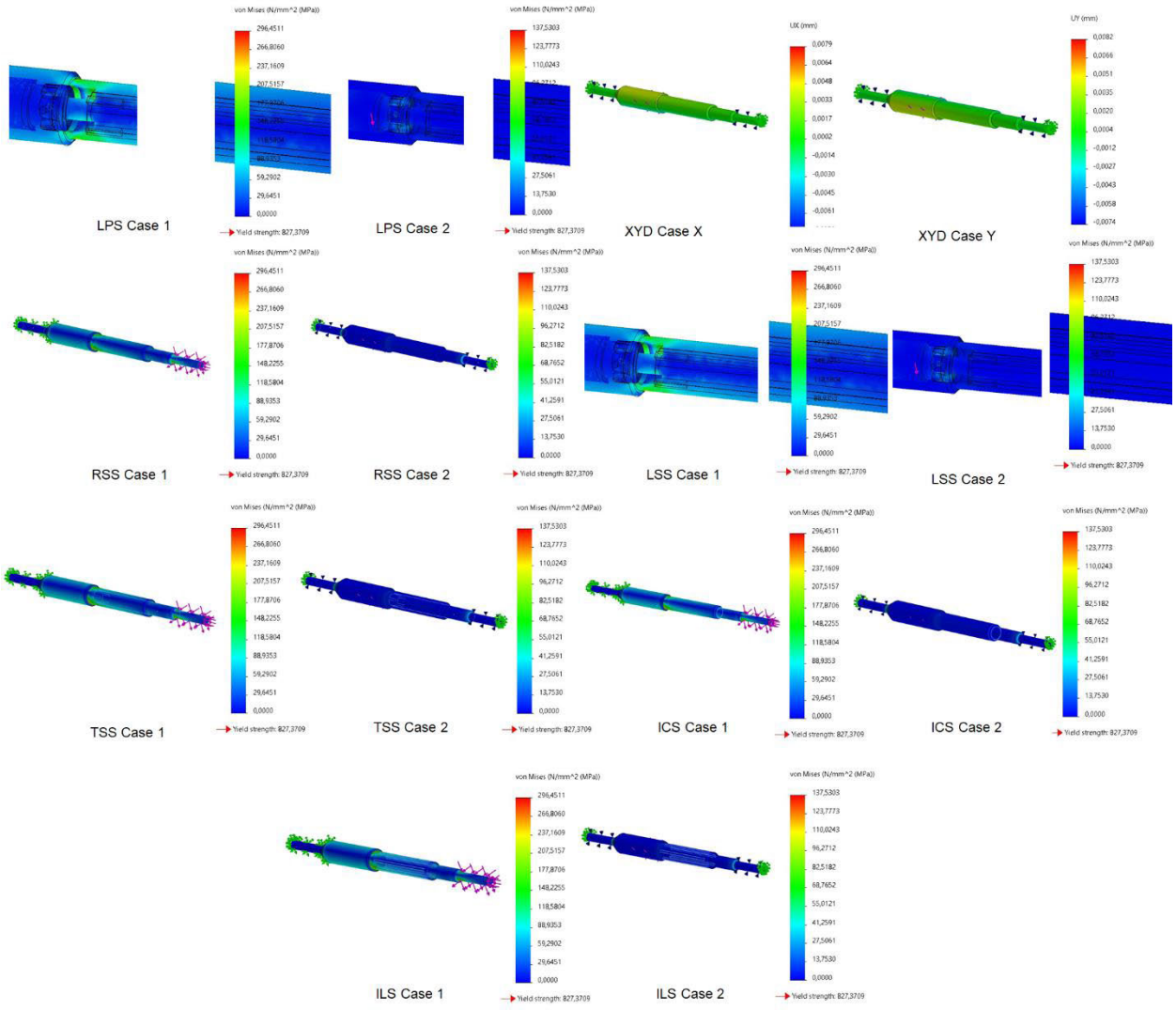


**FIGURE 15.** The Analysis Results of NSGA II.

DESIGN VARIABLE

$$X(CT, HOD, HID, LPD, LD, SW, SH, SL, SN, CH, CUD) \quad (5)$$

## III. RESULTS AND DISCUSSION

The obtained results are discussed in this section. First of all, twelve different MCGR models given in Table 3 are analyzed and the maximum stress and displacements on fourteen control points are logged. An example of analysis results for L12 Exp. 1 is given in Figure 10.

In Figure 11, the obtained plot box as a result of the mechanical analysis is given for all experiments in L12. Using the data in L12 and Figure 11, the relationship between the design parameters and factors according to DoE is given in Figure 12. Here it can be seen that the parameter relationships change between Case 1 and Case 2. For example, in LPS Case 1, CT, LPD, and CH dominate, while in the same stress analysis for Case 2, the effect of CT, LD, and CH decreases, but the effect of SL, SN, and HID increases. This indicates that different dynamics are effective in both cases. It is clear that the situation is not so clear for ICS and that CUD, which dominates this stress value, is at a very high level in both cases. The effect of Lead Diameter is high on all stress and displacement values. At the same time, it can be said that CT has a significant effect on the stress on the lead screw.

The obtained coefficients for the 14 control factors as a result of linear regression show that the maximum error obtained as a result of the regression is 5%. The obtained plot matrix as a result of the optimization performed using NSGA II is shown in Figure 13. Another plot matrix for MOPSO is shown in Figure 14. The optimal design

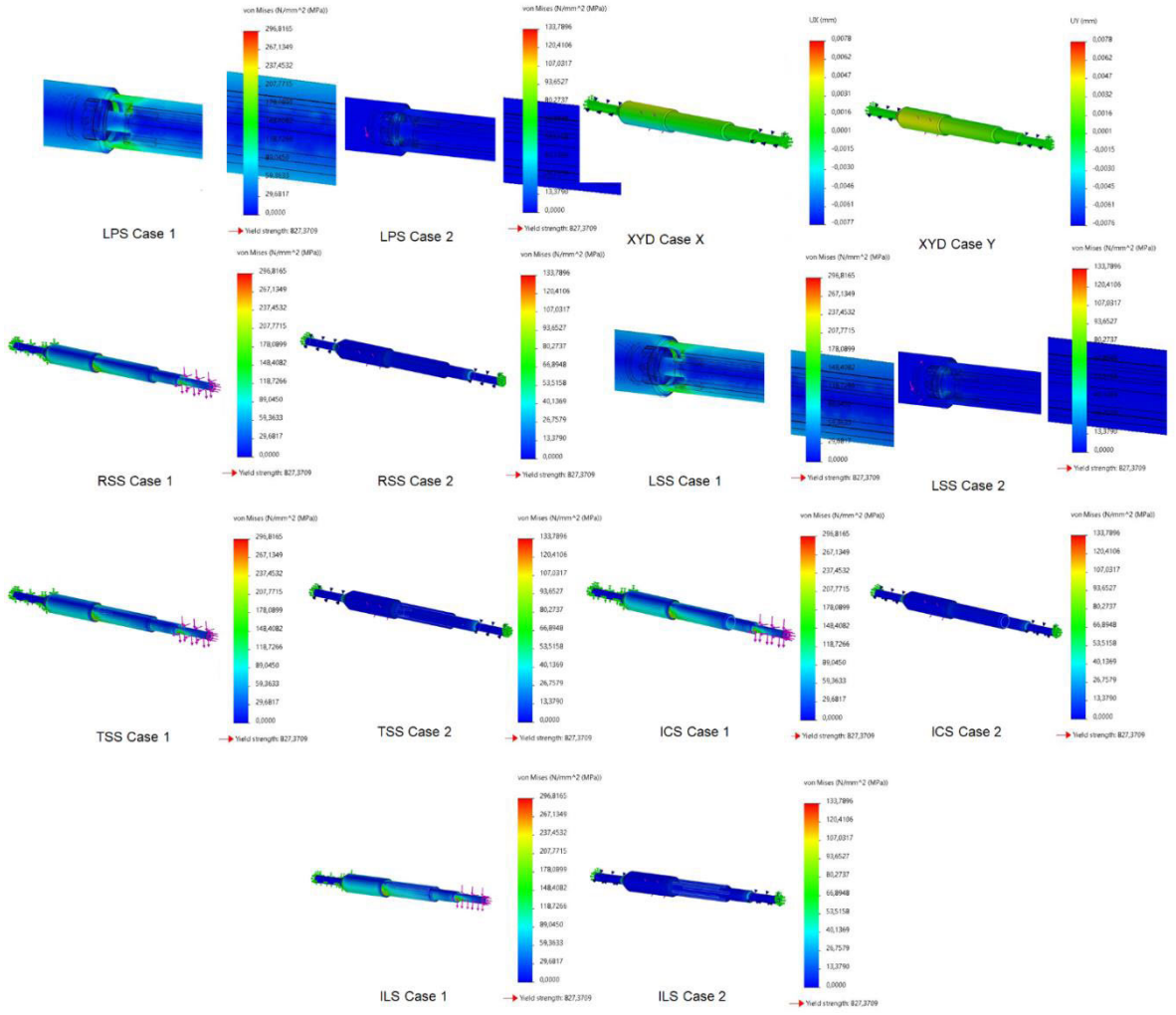


**FIGURE 16.** The Analysis Results of MOPSO.

parameters obtained within the scope of the multi-objective are given in Table 4.

As seen here, the non-dominated solutions for the eleven parametric states are defined for a total of 14 control points and 7 control points for each case, and the median and optimal points for these solutions are shown. Non-dominated solutions are sets of optimal solutions that do not dominate all other parameters. A scatter plot matrix, as shown in Figures 13 and 14, is a reduced graph for examining a 14-dimensional solution space in a two-dimensional way. This allows for a comparison of the optimal solution led by NSGA II and MOPSO with stresses and displacements.

The histograms in the main diagonal of the figure show the concentration of fitness values calculated for each metric. From here, it can be examined which range the solution set shows concentration for the relevant parameter. For example, the solutions for LPS Case 1 concentrate in the range of 100-150 Mpa while they are evenly distributed between 10 and 60 for LPS Case 2. The optimal solution points shown with a star on the graphs are seen to be in these concentration zones.

The graphs at the intersection of rows and columns in the plot matrix graphics show the correlations between the row and column variables. One of the notable results here is the linear correlation between ICS Case 1 and ICS Case 2. Therefore, the Pareto face in the graph is seen as a single point. There is also a strong linear correlation between XYD Case X and XYD Case Y in a similar but more aggressive way. This shows that both variables are affected by the solutions in the same way. It is also seen that the correlations of the pairs that can be observed linearly are correlated with the other parameters.

When compared with Figure 14, it is seen that the standard deviation of the solution space proposed by the NSGA II algorithm is lower than the solution space led by MOPSO. This may be interpreted as the reason that the NSGA II algorithm

**TABLE 7. The overall assessments.**

| Estimated Results -vs- Analysis Results Correlation | | | L12 Exp.1. (MCGR) -vs- Estimated Results | L12 Exp.1. (MCGR) -vs- Analysis Results |
|---|---|---|---|---|
| | MAPE (%) | Improvement | MAPE (%) | MAPE (%) |
| NSGA II | 14% | NSGA II | 34% | %32 |
| MOPSO | 10% | MOPSO | 18% | %30 |

uses the non-dominated sorting method as an elitist selection method. In the MOPSO results, strong linear relationships also appear at similar points.

Table 4 shows the optimal solution proposals led by the two algorithms. The greatest difference between the two solutions is seen in Slider height (SH) Slider width (SW) and HOD. In addition, the distance between the two parametric vectors is less than 1%.

The mechanical analysis results of the solution architecture proposed by NSGA II, seen in Figure 15, are shown in Table 5.

The results of the analysis done with the results suggested by the MOPSO model are seen in Table 6. Here, there is a difference of approximately 8-10% between the LPS and ICS values for the model analyses suggested by the NSGA II algorithm. The difference in the other variables is clearly very small.

The obtained stress and displacement because of mechanical analysis are shown in Figure 15 for NSGA II and Figure 16 for MOPSO. The maximum stress and displacement results obtained in the analyzes are given in Table 5 for NSGA II and in Table 6 for MOPSO. Considering the analysis and optimization, the findings regarding the general assessments and correlation results are given in Table 7. As can be seen here, the correlation values estimated and analyzed with both optimization models are given in the second column. When compared to the analysis results, the MAPE (Mean Absolute Percentage Error) for NSGA is 14%, and for MOPSO it is 10%. This shows that the success rates of the prediction models are 86% and 90% respectively. The section on improvements after optimization compares the results of the first experiment with the optimization results. This result shows that both algorithms have positively impacted the results of the recommended optimum solutions.

## IV. CONCLUSION

In this study, the use of a magnetically controlled growing rod (MCGR) for the treatment of scoliosis is analyzed. The common mechanical issues associated with MCGR are explored and efforts are made to find solutions for improvement. After the treatment, the MCGR removed from a patient is a tear downed, and a solid model (CAD) is created and geometrically parameterized. Here MCGR is separated into eleven different parameters. Considering the mechanical problems experienced, fourteen control points are determined for mechanical analysis. Then, it is decided that the MCGR modeled for eleven parameters and two levels using the DoE method should be subjected to the L12 orthogonal experimental array. Experiments in L12 are carried out and stress and displacement observation taken from fourteen control points are recorded. Linear regression-based fitness functions are created with the experimental combinations in L12 and the obtained data because of the mechanical analysis. Stress and displacements on MCGR are tried to be minimized with both NSGA II and MOPSO by using the created fitness functions. The obtained design models with NSGA II and MOPSO are reanalyzed, and the results are recorded. The findings show that a quite regression is performed with the results of the analysis of the fitness functions, with an accuracy of 14% for NSGA II and 10% for MOPSO. In addition, considering the fitness functions in L12 Exp.1, it is seen that there is an improvement of 34% for NSGA II and 18% for MOPSO. Moreover, the obtained findings as a result of mechanical analyzes show an improvement of 32% in NSGA II and 30% in MOPSO compared to L12 Exp.1. It can be deduced from the analysis results that the newly manufactured MCGR takes into consideration the design parameters calculated using both multiobjective optimization algorithms, is more resilient against mechanical complications when the stress and displacement parameters established at the control points are considered. This will reduce the negative impact of these mechanical complications on patients and treatment processes. The optimization process can be confirmed through the performance of durability tests on the MCGR produced utilizing the design parameters established in this study.

## REFERENCES

[1] J. A. Harris, O. H. Mayer, S. A. Shah, R. M. Campbell, and S. Balasubramanian, "A comprehensive review of thoracic deformity parameters in scoliosis," *Eur. Spine J.*, vol. 23, no. 12, pp. 2594–2602, Dec. 2014.
[2] H. Shakil, Z. A. Iqbal, and A. H. Al-Ghadir, "Scoliosis: Review of types of curves, etiological theories and conservative treatment," *J. Back Musculoskeletal Rehabil.*, vol. 27, no. 2, pp. 111–115, Apr. 2014.
[3] R. M. Kliegman, R. E. Behrman, H. B. Jenson, and B. M. Stanton, "*Nelson Textbook of Pediatrics E-Book*. Amsterdam, The Netherlands: Elsevier, 2007.
[4] F. Altaf, A. Gibson, Z. Dannawi, and H. Noordeen, "Adolescent idiopathic scoliosis," *BMJ*, vol. 346, Apr. 2013, Art. no. f2508.
[5] H. Kim, H. S. Kim, E. S. Moon, C.-S. Yoon, T.-S. Chung, H.-T. Song, J.-S. Suh, Y. H. Lee, and S. Kim, "Scoliosis imaging: What radiologists should know," *Radiographics*, vol. 30, no. 7, pp. 1823–1842, Nov. 2010.
[6] A. Thuaimer, M. Niknejad, and L. Lustosa. *Cobb Angle. RID-23612*. Accessed: Dec. 11, 2022. [Online]. Available: https://Radiopaedia.org, doi: 10.53347/rID-23612.
[7] B. A. Williams et al., "Development and initial validation of the classification of early-onset scoliosis (C-EOS)," *J. Bone Joint Surg.*, vol. 96, no. 16, pp. 1359–1367, 2014.
[8] V. Cunin, "Early-onset scoliosis—Current treatment," *Orthopaedics Traumatol. Surg. Res.*, vol. 101, no. 1, pp. S109–S118, 2015.
[9] Y.-B. Zhang and J.-G. Zhang, "Treatment of early-onset scoliosis: Techniques, indications, and complications," *Chin. Med. J.*, vol. 133, no. 3, pp. 351–357, 2020.
[10] L. A. Karol, C. Johnston, K. Mladenov, P. Schochet, P. Walters, and R. H. Browne, "Pulmonary function following early thoracic fusion in non-neuromuscular scoliosis," *J. Bone Joint Surg.*, vol. 90, no. 6, pp. 1272–1281, Jun. 2008.

[11] M. G. Vitale, H. Matsumoto, M. R. Bye, J. A. Gomez, W. A. Booker, J. E. Hyman, and D. P. Roye Jr., "A retrospective cohort study of pulmonary function, radiographic measures, and quality of life in children with congenital scoliosis: An evaluation of patient outcomes after early spinal fusion," *Spine*, vol. 33, no. 11, pp. 1242–1249, May 2008.

[12] M. Takaso, H. Moriya, H. Kitahara, S. Minami, K. Takahashi, K. Isobe, M. Yamagata, Y. Otsuka, Y. Nakata, and M. Inoue, "New remote-controlled growing-rod spinal instrumentation possibly applicable for scoliosis in young children," *J. Orthopaedic Sci.*, vol. 3, no. 6, pp. 336–340, Nov. 1998.

[13] K. M.-C. Cheung, J. P.-Y. Cheung, D. Samartzis, K.-C. Mak, Y.-W. Wong, W.-Y. Cheung, B. A. Akbarnia, and K. D.-K. Luk, "Magnetically controlled growing rods for severe spinal curvature in young children: A prospective case series," *Lancet*, vol. 379, no. 9830, pp. 1967–1974, May 2012.

[14] J. P. Y. Cheung, P. Cahill, B. Yaszay, B. A. Akbarnia, and K. M. Cheung, "Update on the magnetically controlled growing rod: Tips and pitfalls," *J. Orthopaedic Surg.*, vol. 23, no. 3, pp. 383–390, Dec. 2015.

[15] J. P. Y. Cheung and K. M. Cheung, "Current status of the magnetically controlled growing rod in treatment of early-onset scoliosis: What we know after a decade of experience," *J. Orthopaedic Surg.*, vol. 27, no. 3, Sep. 2019, Art. no. 230949901988694.

[16] C. S. Jones, O. M. Stokes, S. B. Patel, A. J. Clarke, and M. Hutton, "Actuator pin fracture in magnetically controlled growing rods: Two cases," *Spine J.*, vol. 16, no. 4, pp. e287–e291, Apr. 2016.

[17] G. La Rosa, L. Oggiano, and L. Ruzzini, "Magnetically controlled growing rods for the management of early-onset scoliosis: A preliminary report," *J. Pediatric Orthopaedics*, vol. 37, no. 2, pp. 79–85, Mar. 2017.

[18] A. M. Heydar, S. Sirazi, and M. Bezer, "Magnetic controlled growing rods as a treatment of early onset scoliosis: Early results with two patients," *Spine*, vol. 41, no. 22, pp. E1336–E1342, 2016.

[19] A. M. Heydar, S. Şirazi, E. Okay, G. Kiyak, and M. Bezer, "Short segment spinal instrumentation in early-onset scoliosis patients treated with magnetically controlled growing rods," *Spine*, vol. 42, no. 24, pp. 1888–1894, Dec. 2017.

[20] A. M. Heydar, E. Okay, S. Sirazi, A. E. Yenigul, G. Kiyak, T. Balikci, and M. Bezer, "Do magnetically controlled growing rods stimulate longitudinal vertebral growth in early-onset scoliosis patients?" *World Neurosurg.*, vol. 141, pp. e844–e850, Sep. 2020.

[21] T. Odent, B. Ilharreborde, L. Miladi, N. Khouri, P. Violas, J. Ouellet, V. Cunin, J. Kieffer, K. Kharrat, and F. Accadbled, "Fusionless surgery in early-onset scoliosis," *Orthopaedics Traumatol. Surg. Res.*, vol. 101, pp. S281–S288, Oct. 2015.

[22] V. C. Panagiotopoulou, S. K. Tucker, R. K. Whittaker, H. S. Hothi, J. Henckel, J. J. H. Leong, T. Ember, J. A. Skinner, and A. J. Hart, "Analysing a mechanism of failure in retrieved magnetically controlled spinal rods," *Eur. Spine J.*, vol. 26, no. 6, pp. 1699–1710, Jun. 2017.

[23] P. R. P. Rushton, S. L. Smith, L. Forbes, A. J. Bowey, M. J. Gibson, and T. J. Joyce, "Force testing of explanted magnetically controlled growing rods," *Spine*, vol. 44, no. 4, pp. 233–239, Feb. 2019.

[24] U. Demir and M. C. Akuner, "Elektrikli bir araç için tekerlek içi asenkron motorun tasarım ve optimizasyonu," *Gazi Üniversitesi Mühendislik Mimarlık Fakültesi Dergisi*, vol. 33, no. 4, pp. 1517–1530, Dec. 2018, doi: 10.17341/gazimmfd.416448.

[25] U. Demir and M. C. Akuner, "Using Taguchi method in defining critical rotor pole data of LSPMSM considering the power factor and efficiency," *Tehnicki Vjesnik*, vol. 24, no. 2, pp. 347–353, 2017, doi: 10.17559/TV-20140714225453.

[26] U. Demir, "Taşıtlarda katlanabilir koltuk sistemleri için selonoid Aktüatör tasarım ve analizi," *Int. J. Adv. Eng. Pure Sci.*, vol. 32, no. 2, pp. 158–171, Jun. 2020, doi: 10.7240/jeps.586258.

[27] Z. K. Kocabicak and U. Demir, "Design and optimization of an electromechanical actuator for the latch of a foldable vehicle seat," *Mater. Test.*, vol. 62, no. 7, pp. 749–755, 2021, doi: 10.3139/120.111539.

[28] U. Demir, "Improvement of the power to weight ratio for an induction traction motor using design of experiment on neural network," *Electr. Eng.*, vol. 103, no. 5, pp. 2267–2284, Oct. 2021, doi: 10.1007/s00202-020-01204-2.

[29] U. Demir, "IM to IPM design transformation using neural network and DoE approach considering the efficiency and range extension of an electric vehicle," *Electr. Eng.*, vol. 104, no. 2, pp. 1141–1152, Apr. 2022, doi: 10.1007/s00202-021-01378-3.

[30] M. Pourkarimi, U. Demır, and M. C. Akuner, "Neural network approach for E-motor development," in *Proc. 8th Int. Conf. Control, Decis. Inf. Technol. (CoDIT)*, May 2022, pp. 1091–1095, doi: 10.1109/CoDIT55151.2022.9804105.

[31] J. T. Knight, D. J. Singer, and M. D. Collette, "Testing of a spreading mechanism to promote diversity in multi-objective particle swarm optimization," *Optim. Eng.*, vol. 16, pp. 279–302, Jun. 2015, doi: 10.1007/s11081-014-9256-8.

[32] S. G. Kontogiannis and M. A. Savill, "A generalized methodology for multidisciplinary design optimization using surrogate modelling and multifidelity analysis," *Optim. Eng.*, vol. 21, pp. 723–759, May 2020, doi: 10.1007/s11081-020-09504-z.

[33] Ş. Aslan, "Mathematical model and a variable neighborhood search algorithm for mixed-model robotic two-sided assembly line balancing problems with sequence-dependent setup times," *Optim. Eng.*, 2022, doi: 10.1007/s11081-022-09718-3.

[34] G. Petelin, M. Antoniou, and G. Papa, "Multi-objective approaches to ground station scheduling for optimization of communication with satellites," *Optim. Eng.*, vol. 24, pp. 147–184, Mar. 2021, doi: 10.1007/s11081-021-09617-z.

[35] S. C. Caraballo and R. A. Fernandez, "A performance-based design framework for enhancing decision-making at the conceptual phase of a motorcycle rear suspension development," *Optim. Eng.*, vol. 21, pp. 1283–1317, Dec. 2020, doi: 10.1007/s11081-019-09475-w.

[36] C. Thakar, D. C. Kieser, M. Mardare, S. Haleem, J. Fairbank, and C. Nnadi, "Systematic review of the complications associated with magnetically controlled growing rods for the treatment of early onset scoliosis," *Eur. Spine J.*, vol. 27, no. 9, pp. 2062–2071, Sep. 2018.

[37] J. P. Y. Cheung, K. K. L. Yiu, D. Samartzis, K. Kwan, B.-B. Tan, and K. M. C. Cheung, "Rod lengthening with the magnetically controlled growing rod," *Spine*, vol. 43, no. 7, pp. E399–E405, Apr. 2018.

[38] K. H. Teoh, A. N. Moideen, K. Mukherjee, S. Kamath, S. H. James, A. Jones, J. Howes, P. R. Davies, and S. Ahuja, "Does the external remote controller's reading correspond to the actual lengthening in magnetic-controlled growing rods?" *Eur. Spine J.*, vol. 29, no. 4, pp. 779–785, Apr. 2020.

[39] K. H. Teoh, C. von Ruhland, S. L. Evans, S. H. James, A. Jones, J. Howes, P. R. Davies, and S. Ahuja, "Metallosis following implantation of magnetically controlled growing rods in the treatment of scoliosis: A case series," *Bone Joint J.*, vols. 98–B, no. 12, pp. 1662–1667, Dec. 2016.

[40] C. Yilgor, A. Efendiyev, F. Akbiyik, G. Demirkiran, A. Senkoylu, A. Alanay, and M. Yazici, "Metal ion release during growth-friendly instrumentation for early-onset scoliosis: A preliminary study," *Spine Deformity*, vol. 6, no. 1, pp. 48–53, Jan. 2018.

[41] J. P. Y. Cheung, T. Zhang, C. Bow, K. Kwan, K. Y. Sze, and K. M. C. Cheung, "The crooked rod sign: A new radiological sign to detect deformed threads in the distraction mechanism of magnetically controlled growing rods and a mode of distraction failure," *Spine*, vol. 45, no. 6, pp. E346–E351, 2020.

[42] T. J. Joyce, S. L. Smith, P. R. P. Rushton, A. J. Bowey, and M. J. Gibson, "Analysis of explanted magnetically controlled growing rods from seven U.K. spinal centers," *Spine*, vol. 43, no. 1, pp. E16–E22, Jan. 2018.

[43] J. Z. Wei, H. S. Hothi, H. Morganti, S. Bergiers, E. Dal Gal, D. Likcani, J. Henckel, and A. J. Hart, "Mechanical wear analysis helps understand a mechanism of failure in retrieved magnetically controlled growing rods: A retrieval study," *BMC Musculoskeletal Disorders*, vol. 21, no. 1, pp. 1–11, Dec. 2020.

**UĞUR DEMİR** received the Ph.D. degree in mechatronics engineering from Marmara University, in 2018. He is currently an Associate Professor with the Department of Mechatronics Engineering, Marmara University. He has extensively worked on the development of novel electrical machine technologies for electric vehicle traction operations and mechatronics systems. His research interests include the electromagnetic design of electrical machines, design optimization, artificial neural network applications, autonomous driving, and advanced driving technologies.

**GAZI AKGÜN** was born in Denizli, Turkey, in 1982. He received the B.Sc. degree in electrical education from Dicle University, Batman, Turkey, in 2004, and the M.Sc. and Ph.D. degrees in mechatronics engineering from Marmara University, Istanbul, in 2015 and 2019, respectively.

From 2005 to 2021, he was a Vocational Technical Teacher in various cities around Turkey for the National Educational Ministry. Currently, he is an Assistant Professor with the Department of Mechatronics Engineering, Marmara University. His research interests include adaptive control, predictive control, and AI-supported intelligent control systems, particularly in the fields of biomechatronics and rehabilitation robotics.

**SITKI KOCAOĞLU** was born in Ankara, Turkey, in 1984. He received the B.S. degree in electrical and electronics engineering from Selçuk University, Konya, in 2007, the M.S. degree in mechanical engineering from Trakya University, Edirne, in 2013, and the Ph.D. degree in mechatronics engineering from Yıldız Technical University, Istanbul, in 2019.

From 2009 to 2020, he was a Lecturer with Kırklareli University. Since 2020, he has been an Assistant Professor with the Biomedical Engineering Department, Ankara Yıldırım Beyaz*University, Ankara. He is the author of more than 20 articles and holds a patent. His research interests include biomechatronics, innovative prostheses, and artificial intelligence.*

**MD. ERHAN OKAY** received the M.D. degree from Gaziantep University, Gaziantep, Turkey, in 2010. He completed the Orthopedic Residency Program from the Faculty of Medicine, Marmara University, Istanbul, Turkey, in 2017.

**AHMED MAJID HEYDAR** was born in Al-Basrah, Iraq, in 1980. He received the bachelor's degree in medicine and general surgery from the College of Medicine, in 2005.

From 2010 to 2015, he was a Research Fellow with the Orthopedic and Traumatology Department, Medical School, Marmara University, Istanbul, Turkey. His residency thesis was on the early results of magnetic growing rods in the treatment of early-onset scoliosis. Since 2021, he has been an Orthopedic Surgeon with the Esenyurt State Hospital and a Lecturer with the Physiotherapy and Rehabilitation Faculty, Marmara University. He has conducted and published many clinical studies mostly focusing on magnetic growing rods and their application in the medical field. He is a member of the Turkish Orthopaedic and Traumatology Association, the Turkish Spinal Society, and the Society of Turkish-Speaking Countries of Orthopaedic and Traumatology. He was a fellow of the Turkish Orthopedics and Traumatology Training Council and the European Board of Orthopedic and Traumatology (FEBOT), in 2015 and 2016, respectively.

**ERHAN AKDOGAN** (Member, IEEE) received the B.S. degree in electronics and communication engineering from Yıldız Technical University, Istanbul, Turkey, in 1999, and the M.S. and Ph.D. degrees from Marmara University, Turkey, in 2001 and 2007, respectively. From 2008 to 2009, he was a Visiting Researcher with the Biological Systems Engineering Laboratory, Graduate School of Engineering, Hiroshima University. He is currently a Professor with the Mechatronics Engineering Department, Yıldız Technical University.

**ALPER YILDIRIM** was born in Izmir, Turkey, in 1997. He received the B.S. degree in mechatronic engineering from Izmir Katip Celebi University, Izmir. He is currently pursuing the M.Sc. degree with the Mechatronics Engineering Department, Marmara University.

Since 2021, he has been a Research Assistant with the Department of Mechatronics Engineering, Marmara Universiy. His research interest includes control engineering.

**SEVDENUR YAZI** was born in Tekirdag, Turkey, in 1997. She received the B.S. degree in physiotherapy and rehabilitation from Bezmialem University, Istanbul, Turkey, in 2019, and the M.S. degree in anatomy from Marmara University, Istanbul, in 2022, where she is currently pursuing the Ph.D. degree in anatomy.

Since 2019, she has been a Research Assistant with the Department of Anatomy, School of Medicine, Marmara University. Her research interests include human anatomy, neuroscience, scoliosis, neuron morphology in absence epilepsy, and Alzheimer's disease.

Ms. Yazi is a member of the Federation of European Neuroscience Societies.

**BORA DEMİRCİ** received the B.S. degree in mechatronics, robotics, and automation engineering from Kocaeli University, Turkey, in 2017, and the M.Sc. degree in mechatronics engineering from Marmara University, Istanbul, Turkey, in 2022, where he is currently pursuing the Ph.D. degree with the Mechatronics Engineering Department.

He has been an Elite Applications–CAE Application Engineer with TEKYAZ Technological Software, Istanbul. His research interests include CAD, CAE, and CFD analysis.

**ERKAN KAPLANOGLU** (Senior Member, IEEE) is currently an Associate Professor with the Department of Engineering Management and Technology, Mechatronics, The University of Tennessee at Chattanooga (UTC). He founded the Biomechatronics and Assistive Technology Laboratory (BioAstLab), in 2019. The establishment of this laboratory has led to collaborations with the departments of biomedical and medical at other partner higher education institutions. His research interests include robotics, biomechatronics, automation, and Industry 4.0. He is a Senior Member of the International Association of Engineers (IAENG) and the European Embedded Control Institute (EECI).